JJEE

Volume 10 | Number 2 | June 2024 | Pages 240-252

Jordan Journal of Electrical Engineering

ISSN (print): 2409-9600, ISSN (online): 2409-9619

Homepage: jjee.ttu.edu.jo

Load Frequency Control and Optimization of Load Allocation for Multi-Area Power System with Electric Vehicle Charging Load

Najmuddin M. Jamadar[1*], Suhani Jamadar[2], H. T. Jadhav[3]

[1, 2] Electrical Engineering Department, Yashoda Technical Campus, Satara, India
E-mail: najmuddinjamadar@gmail.com
[3] Faculty of Science and Technology, SNDT University, Mumbai, India

Received: Jul 08, 2023 *Revised: Sep 18, 2023* *Accepted: Sep 24, 2023*

***Abstract*—** The integration of electric vehicles (EVs) into power systems has introduced new challenges for load frequency control due to the additional charging load they impose. This research article investigates the design and analysis of automatic load frequency control in a two-area power system, considering the presence of EV charging load. The study employs Artificial Neural Network (ANN) based PI control to manage both traditional load demand and the dynamic charging requirements of EVs. Maintaining a stable power system frequency and balancing generation with the EV charging load have become crucial tasks. Automatic Generation Control (AGC) or Load Frequency Control (LFC) systems need to adapt and account for the variability and uncertainty associated with EV charging patterns. The integration of ANN-based PI control provides an intelligent and adaptive approach to address these challenges. Using MATLAB, a power system model is simulated to evaluate the effectiveness of the proposed control scheme. This investigation conducts a comparative analysis of the system's frequency responses under various scenarios, including different EV charging load profiles. It highlights the benefits and challenges of utilizing ANN-based PI control to manage the combined load of traditional demand and EV charging. Moreover, the load distribution among the distribution stations varied from 0.08% to 12.50% when compared between particle swarm optimization and genetic algorithm, respectively. By considering the dynamic interaction between power system operation and EV charging, this research aims to enhance the reliability, efficiency and sustainability of power systems in the context of evolving transportation trends and the increasing electrification of vehicles.

***Keywords*—** Load frequency control; Electric vehicle charging load; Optimization; Load allocation; Two-area power system.

Nomenclature

ACE	Area correction error	ΔPi	Tie-line power dynamics
ADD	Additional symbols and terms	ΔPrefi	Control action in ANN
ANN	Artificial neural network	ΔUi	Prime mover and generation dynamics
CA	Control area	α	Load characteristic coefficient
CPF	Contract participation factor	β	Governor gain
DPM	Disco participation matrix	δ	Rotor angle
EV	Electric vehicle	δ0	Equilibrium rotor angle
GA	Genetic algorithm	ε	Tolerance
GENCO	Generation station	θ	Totor angle
PSO	Particle swarm optimization	η	Learning rate
pu	Per unit	μ(Δf(t))	Fuzzy logic controller

* Corresponding author
DOI: https://doi.org/10.5455/jjee.204-1688815488

STD	Standard deviation	ω	Actual speed
ωref	Reference frequency	ωref	Reference speed
Δf	Frequency deviation	ωs	Synchronous speed
ΔP_ec	EV load control equation	$\Delta \omega i$	Speed deviation
ΔP_gc	Generator control equation		

1. INTRODUCTION

In recent years, the integration of electric vehicles (EVs) into the power grid has introduced new challenges and opportunities for the reliable operation of power systems. The increasing adoption of EVs, coupled with their charging load, adds an additional layer of complexity to the already existing load demand and generation control issues. Maintaining a stable power system frequency while efficiently managing the charging requirements of EVs has become a critical aspect of power system operation. Automatic load frequency control systems, which traditionally focus on balancing generation and demand, must now adapt to incorporate the charging load of EVs. This integration requires careful coordination to ensure that the charging demand is met while maintaining the stability and reliability of the power system. The charging load of EVs can have a significant impact on power system dynamics, especially during peak demand periods.

The incorporation of electric vehicles (EVs) into power systems has sparked significant interest due to its implications for Load Frequency Control (LFC). This review delves into key studies that illuminate the complex relationship between EVs and LFC, showcasing their interplay and identifying research gaps that underscore our paper's significance.

Khan et al. [1] delved into the participation of EVs in LFC using mixed $H2/H\infty$ control. Their study revealed the potential of EVs as controllable resources for enhancing frequency stability in dynamic power systems. Khalil et al. [2] explored the impact of time delay on LFC in microgrids with plug-in EVs. This study emphasized the need to consider EV dynamics when designing LFC strategies. Farooq et al. [3] extended LFC considerations to multi-source electrical power systems integrated with solar-thermal and EVs. Their research highlighted the challenges and opportunities posed by renewable energy and EV integration in LFC. Pham and Trinh [4] introduced LFC strategies for power systems incorporating EVs and diverse transmission links. Their study showcased the integration of advanced control techniques to manage the evolving dynamics of modern power grids. Arya [5] investigated the effect of EVs on LFC in interconnected thermal and hydrothermal power systems. The study emphasized the role of control strategies in maintaining frequency stability in evolving power scenarios. Zhang et al. [6] focused on real-time adjustments of LFC based on the controllable energy of EVs. Their research shed light on the potential of EVs to provide ancillary services for frequency regulation. Dutta and Prakash [7] explored the utilization of EVs and renewable energy sources for LFC in deregulated power systems using an emotional controller. Their study introduced unconventional control methods for dynamic power systems. Tang et al. [8] proposed an intelligent LFC strategy utilizing GrADP for island smart grids with EVs and renewable resources. This work illustrated the adaptability of AI-based control approaches in addressing complex power system dynamics. Naveed et al. [9] studied the impact of EV aggregator communication time delay on stability regions and delay margins in LFC. Their work highlighted the significance of communication dynamics in shaping LFC performance. Khooban et al. [10] presented a new LFC strategy for microgrids considering EVs. This study emphasized tailored strategies for managing frequency control in evolving energy paradigms. Aravindh et al. [11] designed an observer-based non-fragile LFC strategy for power systems with EVs. This research contributed to the development of robust control techniques for managing EV-related dynamics.

1.1. Research Gaps and Implications

While these studies collectively enhance our understanding of EVs' impact on LFC, a clear research gap surfaces: the integration of EVs within the broader context of LFC. The current literature lacks a comprehensive exploration of how EVs interact with LFC strategies. This research gap underscores the importance of our study, which aims to bridge this gap and provide insights into effective strategies for integrating EVs into LFC frameworks. In response to this research gap, our study endeavors to address the intricate relationship between EVs and Load Frequency Control. By shedding light on this interaction, we aim to contribute to a comprehensive understanding of power system dynamics, paving the way for innovative strategies that optimize frequency control in the presence of EVs.

2. MATHEMATICAL MODELLING

Modeling a power system with load frequency control involves simulating the system's behavior while considering the automatic control mechanisms that regulate the frequency in response to load changes. Key aspects include modeling governor systems on power generators, representing various load types and their response to frequency deviations, simulating automatic generation control (AGC) for coordinated frequency regulation, analyzing system dynamics and stability, evaluating frequency response performance, tuning controller parameters for optimal operation, and incorporating ancillary services. Load frequency control is crucial for maintaining frequency stability and reliable power system operation. Modeling enables the assessment of dynamic behavior, control performance, and response under different conditions and disturbances. The fundamental equation describes the rate of change of system frequency ($\frac{df}{dt}$) is related to the mismatch between generation and load. The rate of change of frequency is proportional to the net difference between mechanical power input to the generators(P_{mi}), electrical power demand (P_{di}), and a damping term:

$$\frac{df}{dt} = \frac{1}{2H}\left(\sum_{i=1}^{N} P_{mi}(t) - \sum_{i=1}^{N} P_{di}(t) - D(f - f_0) - P_{EV}(t)\right) \tag{1}$$

Where:

$\frac{df}{dt}$ is the rate of change of frequency, H is the total system inertia, N is the number of generators, $P_{mi}(t)$ is the mechanical power input of generator i at time t, $P_{di}(t)$ is the electrical power demand of load i at time t, D is the damping coefficient; f is the actual frequency, f_0 is the nominal (desired) frequency and $P_{EV}(t)$ is the electric vehicle charging load at time t.

With Eq. (1) [2], we account for the impact of the EV charging load on the rate of change of frequency. When $P_{EV}(t)$ is positive indicating EVs are charging and drawing power from the grid, it adds to the electrical demand ($\sum_{i=1}^{N} P_{di}(t)$), which can result in a decrease in system frequency. Conversely, when $P_{EV}(t)$ is negative indicating EVs are discharging or not drawing power from the grid, it subtracts from the electrical demand, potentially leading to an increase in system frequency.

2.1. Power System Model

Consider a multi-area power system comprising N interconnected areas. Each area includes generators, loads, and EV charging stations. The power system is represented by the following variables:

Generator Parameters: Generator parameters are crucial in load frequency control (LFC) for regulating the frequency of a power system. The key parameters include governor droop, governor gain, governor and turbine time constants, generation limits, and rate limiting. Governor droop determines the generator's sensitivity to frequency deviations, while the gain determines the proportional relationship between frequency deviation and output change. Time constants represent the response time of the governor and turbine. Generation limits ensure generators operate within technical limits.

Rate limiting prevents abrupt changes in output. Accurate modeling of these parameters is vital for realistic simulations and maintaining frequency stability within acceptable limits in LFC. Generation Power: P_gi(t), where i is the index of the generator in area A. Governor Control: ΔP_gi(t), representing the change in generation power due to governor control action.

2.2. Load Parameters

In load frequency control (LFC), load parameters, including electric vehicle (EV) charging, are important factors to consider. Key load parameters include load characteristics, load shedding, demand response, EV charging, load forecasting, load ramp rates, and load aggregation. Load characteristics capture the behavior of different load types in response to frequency deviations. Load shedding and demand response mechanisms prioritize and adjust load consumption during frequency emergencies.

EV charging parameters encompass charging profiles, infrastructure availability, and the impact on load demand and frequency fluctuations. Accurate load forecasting, considering load ramp rates and load aggregation techniques enhances LFC modeling. Integrating EV charging parameters and load dynamics in LFC modeling enables effective frequency control and system stability.

The load papramеters utilized in this investigation are L: Traditional Load P_li(t), where i is the index of the load in area A; EV Charging Load: P_evi(t), where i is the index of the EV charging load in area A; Tie Line Power Flow: P_ti(t), where i is the index of the tie line between areas A and B.

2.3. Load Frequency Control Model

The objective of load frequency control is to maintain power system frequency and tie-line power within acceptable limits. The model comprises the following components:

Frequency Deviation: Δf(t), representing the deviation of the system frequency from the nominal value; Generator Control Action: ΔP_gc(t), which adjusts the generation power to match the load demand and restore frequency; EV Load Control Action: ΔP_ec(t), which adjusts the EV charging load to manage the charging demand and frequency deviations.

2.3.1. Control Parameters

Proportional Gain: Kp, determining the strength of the proportional control action. Integral Gain: Ki, determining the strength of the integral control action. Fuzzy Logic

Membership Functions: $\mu(x)$, defining the membership degree of a variable x in a fuzzy set. Control equations are mentioned as follows:

Generator Control Equation:

$$\Delta P\_gc(t) = Kp * (\Delta f(t) + Ki * \int \Delta f(t)\, dt) \quad (2)$$

Eq. (2), describes the connection between the frequency deviation (Δf) and the corresponding adjustment in generator power (ΔP_gc). This adjustment mechanism employs a proportional-integral (PI) control structure, utilizing parameters Kp and Ki, to maintain precise regulation of the system's frequency.

EV Load Control Equation:

$$\Delta P\_ec(t) = \mathrm{FuzzyLogicController}(\Delta f(t)) + \mathrm{ANNController}(\Delta f(t)) \quad (3)$$

Eq. (3) outlines the EV load control equation, in which adjustments (ΔP_ec) are derived through a blend of Fuzzy Logic Controller and Artificial Neural Network (ANN) Controller.

These adjustments are computed concerning the frequency deviation (Δf).

Fuzzy Logic Controller:

$$\Delta P\_ec(t) = \mathrm{defuzzify}(\mu(\Delta f(t)) \quad (4)$$

Eq. (4), signifies the process of translating the fuzzy output representing the adjustment to the electric vehicle load at a given time t, determined based on the degree of membership of the observed frequency deviation (Δf(t)) to linguistic labels, into a precise numerical value for regulating the power system's frequency.

Artificial Neural Network (ANN) Controller:

$$\Delta P\_ec(t) = \mathrm{ANN}(\Delta f(t)) \quad (5)$$

Eq. (5), represents the calculation of the adjustment (ΔP_ec(t)) to the electric vehicle load at a specific time t using an Artificial Neural Network (ANN) controller based on the observed frequency deviation (Δf(t)), enabling intelligent control of the power system.

Tie Line Power Control Equation:

$$P\_ti(t) = P\_gA(t) - P\_gB(t) \quad (6)$$

Eq. (6), computes the tie-line power flow (P_ti(t)) at a given time t as the difference between the generation power of area A (P_gA(t)) and the generation power of area B (P_gB(t)), representing the power exchange between interconnected areas in a power system.

2.3.1.1. Rule Base

Definition of a set of rules that map the input variables to output control actions is represented in Table 1.

Table 1. Fuzzy logic rules.

Rule number	Rule
Rule 1	IF Δf(t) is NB THEN ΔP_ec(t) is Positive
Rule 2	IF Δf(t) is NM THEN ΔP_ec(t) is Positive
Rule 3	IF Δf(t) is ZE THEN ΔP_ec(t) is Zero
Rule 4	IF Δf(t) is PM THEN ΔP_ec(t) is Negative
Rule 5	IF Δf(t) is PB THEN ΔP_ec(t) is Negative

We apply fuzzy logic inference methods, to determine the appropriate control action based on the fuzzy rules and input values. Convert the fuzzy control action into a crisp value using defuzzification methods, such as centroid or weighted average. The output of the fuzzy logic controller, $\Delta P\_ec(t)$, is used as the control action for adjusting the EV charging load to manage the charging demand and frequency deviations.

2.3.1.2. Artificial Neural Network (ANN) Controller

The mathematical model for load frequency control using an Artificial Neural Network (ANN) controller is represented as a set of equations. Here is a simplified mathematical model:

System Dynamics:

The dynamic behavior of the load frequency control system can be described using differential equations. A commonly used model is the two-area power system model: For each area i (i = 1, 2):

Governor Dynamics:

$$\Delta Pci/dt = (1/Tgi)(Pgi - Kpgi\Delta\omega i - Kdigi(d(\Delta\omega i)/dt)) \quad (7)$$

Eq. (7), represents the rate of change of the control signal (ΔPci) for a generator's power output and is determined by factors including the generator's inertia (Tgi), mechanical power input (Pgi), and the governor's proportional (Kpgi) and derivative (Kdigi) control gains.

Turbine-Governor Transfer Function:

$$Pgi = Ktgi(\Delta Prefi - \Delta Ui) \quad (8)$$

Eq. (8), defines the power output (Pgi) of a generator, which depends on the turbine-governor transfer function gain (Ktgi) and the difference between the reference power (ΔPrefi) and the actual power (ΔUi) generated by the generator.

Prime Mover and Generation Dynamics:

$$D(\Delta Ui)/dt = (1/Tdi)(\Delta Pi - \Delta Ui) \quad (9)$$

Eq. (9), represents the rate of change of the internal state variable (ΔUi) of a generator, which depends on the difference between the generated power (ΔPi) and the internal state (ΔUi), with consideration for the governor's time constant (Tdi).

Tie-Line Power Dynamics:

$$D(\Delta Pi)/dt = (1/Tki)(Pci - \Delta Pi - Kpfi(\Delta\omega i - \Delta\omega r)) \quad (10)$$

Eq. (10), describes the rate of change of tie-line power deviation (ΔPi) for time, which is influenced by factors including the difference between the generated power at the control area (Pci), the tie-line power (ΔPi), and the proportional feedback control term, adjusted by the governor's time constant (Tki).

The ANN controller aims to adjust the control action (ΔPrefi) based on system measurements (Δωi, ΔPi) to maintain system frequency within desired limits. The ANN controller maps the input variables (Δωi, ΔPi) to the control action (ΔPrefi) which is represented in Eq. (11).

$$\Delta Prefi = f(\Delta\omega i, \Delta Pi) \quad (11)$$

The function f represents the trained ANN controller, which is represented in Eq. (11) as a set of weighted connections and activation functions within the neural network architecture. The objective of load frequency control is to maintain system frequency within desired limits by adjusting the control action (ΔPrefi). This is achieved by minimizing a performance index, such as the integral of the squared error (ISE):

$$J = \int [\omega ref - \Delta\omega i(t)]^2\, dt \quad (12)$$

where, ωref is the desired reference frequency. Eq. (12), represents a performance index (J) used to evaluate the load frequency control system's effectiveness by integrating the squared deviation of the system's frequency (Δωi(t)) from the reference frequency (ωref) over time.

3. SYSTEM DEVELOPMENT

3.1. System Dynamics

The mathematical model for load frequency control (LFC) involves representing the dynamics of the power system, generator models, control loop, and load models. Here is a simplified mathematical representation.

3.1.1. Frequency Dynamics

The rate of change of system frequency (df/dt) is proportional to the frequency deviation from the nominal value (Δf) and inversely proportional to the total system inertia (H) as shown by Eq. (13).

$$df/dt = -(1/H) * \Delta f \tag{13}$$

3.1.2. Generator Models

Generator Mechanical Dynamics: The mechanical equation of each generator represents the response of the generator's turbine to changes in output. Eq. (14), describes the mechanical dynamics of a generator, where M is the inertia constant, δ represents the rotor angle, Pm is the mechanical power input, Pe is the electrical power output, D is the damping coefficient, and δ0 is the equilibrium rotor angle.

$$M * d^2\delta/dt^2 = Pm - Pe - D * (\delta - \delta 0) \tag{14}$$

where M is the generator's inertia constant, δ is the rotor angle, Pm is the mechanical power input, Pe is the electrical power output, D is the damping coefficient, and δ0 is the equilibrium rotor angle.

3.1.3. Governor Dynamics

Eq. (15) represents the governor dynamics of a generator, with ΔP as the change in generator output, K as the governor droop gain, ωref as the reference speed, ω as the actual speed, β as the governor gain, and Δf as the frequency deviation. A typical governor model is the speed droop model, which is represented as:

$$\Delta P = K * (\omega ref - \omega) - \beta * \Delta f \tag{15}$$

where ΔP is the change in generator output, K is the governor droop gain, ωref is the reference speed, ω is the actual speed, β is the governor gain, and Δf is the frequency deviation.

3.1.4. Control Loop

Control Action:

The control action adjusts the generator output (ΔP) based on the frequency error (Δf). It is represented as:

$$\Delta P = Kc * \Delta f \tag{16}$$

where Kc is the control gain. Eq. (16), represents the control action where ΔP is the change in generator output, Kc is the control gain, and Δf is the frequency deviation used to adjust the generator's output in response to frequency deviations.

3.1.5. Load Models

Load Characteristics: Load characteristics capture the behavior of different types of loads. A simplified model for the load power response to frequency variations is represented as:

$$\Delta Pl = -\alpha * \Delta f \tag{17}$$

where ΔPl is the change in load power, and α is the load sensitivity constant.

Above Eq. (17), describes the change in load power (ΔPl) in response to frequency deviations (Δf), where α is the load sensitivity constant, and it signifies how to load power responds to variations in system frequency.

The equations and control strategies discussed aim to regulate frequency deviations within acceptable limits. While tie-line power control and other aspects are integral to the broader power system operation, our primary focus in the derivation is frequency maintenance, as accurate frequency control is vital for overall power system stability.

3.2. Discom Participation Matrix

The Discom Participation Matrix shown in Fig. 1 is a tool used in power system analysis and planning. It outlines the involvement of distribution companies (Discoms) in various activities related to power system operation. The matrix lists activities/functions and Discoms, indicating the level of participation or responsibility for each activity. It helps define roles and responsibilities, ensures compliance with regulatory frameworks, and promotes coordination among stakeholders. The matrix facilitates efficient power system management and fosters collaboration between Discoms and other entities in the power sector.

In the restructured system, power generation companies (GENCOs) sell electricity to different distribution companies (DISCOs) at competitive prices. This gives DISCOs the freedom to choose which GENCOs they want to enter into contracts with. The contracts may or may not be limited to GENCOs operating within the DISCOs' areas. This flexibility allows for various combinations of GENCO-DISCO contracts to be formed. To facilitate the visualization of these contracts, we introduce the concept of a "DISCO participation matrix" (DPM). The DPM is a matrix that has several rows equal to the number of GENCOs, and several columns equal to the number of DISCOs in the system. Each entry in the matrix represents a fraction of the total electricity load contracted by a DISCO (column) from a specific GENCO (row). Therefore, each entry indicates the proportion of the total contracted load that the DISCO has assigned to a particular GENCO. It is important to note that the sum of all the entries in each column of the DPM is equal to one, as it represents the complete participation of the DISCO in contracts with different GENCOs. The DPM provides a clear representation of the level of involvement of each DISCO in contracts with various GENCOs, which is why it is referred to as the "DISCO participation matrix."

$$\mathbf{DPM} = \begin{array}{r} \\ \textbf{Area 1}\ \begin{array}{c}1\\2\end{array} \\ \textbf{Area 2}\ \begin{array}{c}3\\4\end{array} \end{array} \begin{array}{c} \begin{array}{cccc} 1 & 2 & 3 & 4 \end{array}\ \text{DISCO} \\ \left(\begin{array}{cc|cc} cpf_{11} & cpf_{12} & cpf_{13} & cpf_{14} \\ cpf_{21} & cpf_{22} & cpf_{23} & cpf_{24} \\ \hline cpf_{31} & cpf_{32} & cpf_{33} & cpf_{34} \\ cpf_{41} & cpf_{42} & cpf_{43} & cpf_{44} \end{array}\right) \end{array} \ \text{GENCO}$$

Fig. 1. DISCOM participation Matrix.

where CPF refers to the “contract participation factor”. Suppose that DISCO demands 0.1 pu MW power, out of which 0.025pu MW is demanded from GENCO 1, 0.03puMW from

GENCO 2, 0.035pu MW from GENCO 3, and 0.01puMW from GENCO 4. Then column 3 entries are easily defined as:

$$CPf_{13}=0.025/0.1=0.25, \qquad CPf_{23}=0.03/0.1=0.3$$
$$CPf_{33}=0.035/0.1=0.35, \qquad CPf_{43}=0.01/0.1=0.1$$

4. RESULTS AND DISCUSSION

The model of the platform used for simulation consists of two interconnected control areas (CA). Every CA is represented with one substitute power plant and associated Load frequency controller. Using the proposed control algorithms (Fuzzy Logic and Artificial Neural Network), the frequency deviation of each area and the tie-line power have a good dynamic response in comparison with conventional control. The simulation results of the 13 parameters of the system are drawn in Fig. 2 to Fig. 14 comparing their responses with the proposed controllers. Dynamic Response of LFC with different controllers is represented in Fig. 4 and Fig. 6 which shows reduction in area correction error (ACE).

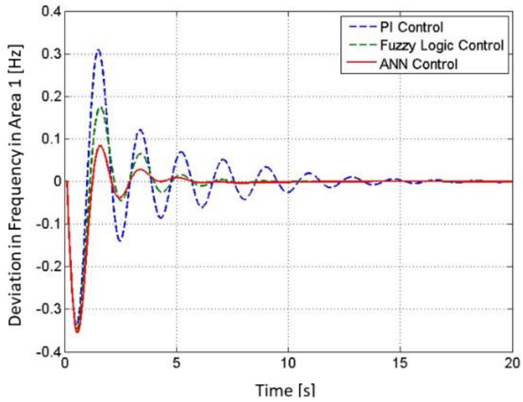

Fig. 2. Deviation of frequency in area 1.

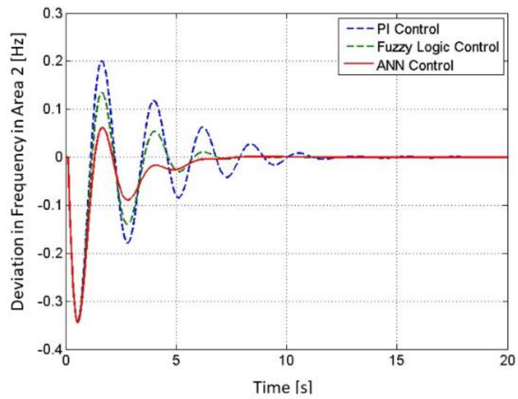

Fig. 3. Deviation of frequency in area 2.

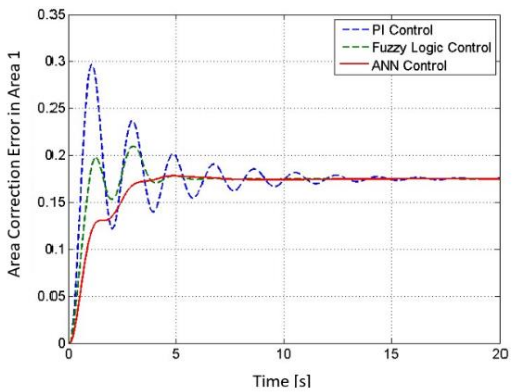

Fig. 4. Deviation of ACE in area 1.

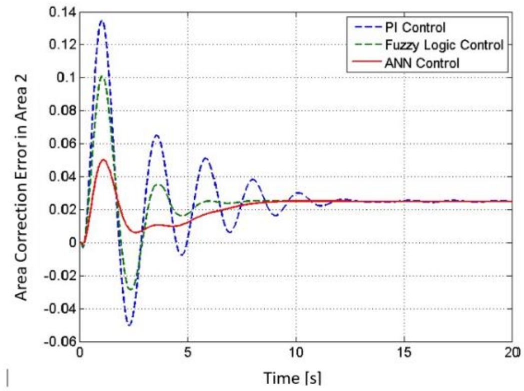

Fig. 5. Deviation of ACE in area 2.

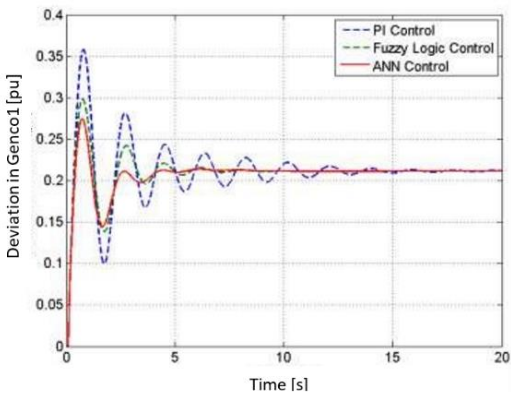

Fig. 6. Deviation of GENCO1 power.

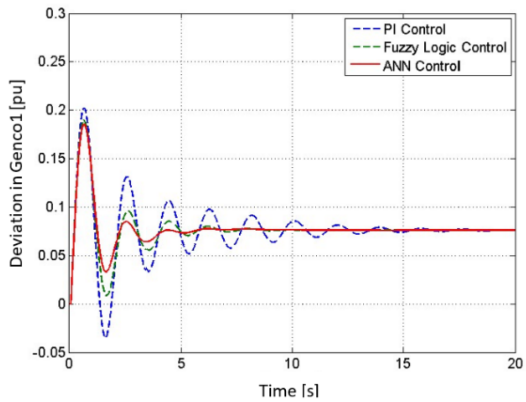

Fig. 7. Deviation of GENCO2 power.

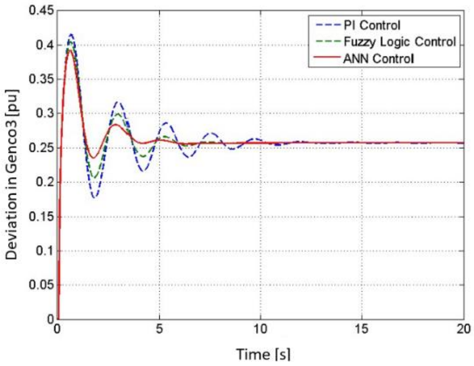

Fig. 8. Deviation of GENCO3 power.

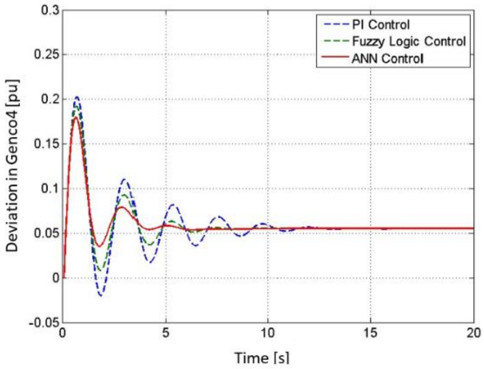

Fig. 9. Deviation of GENCO4 power.

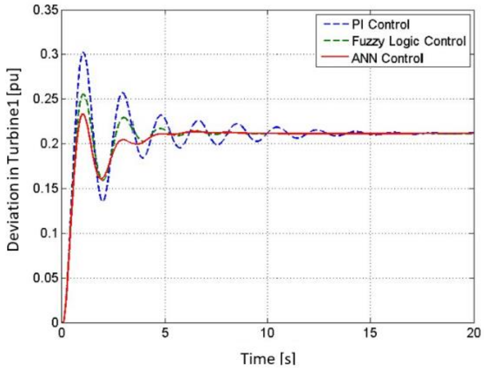

Fig. 10. Deviation of TURBINE1 power.

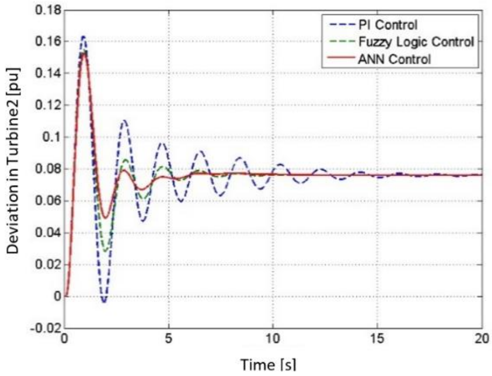

Fig. 11. Deviation of TURBINE2 power.

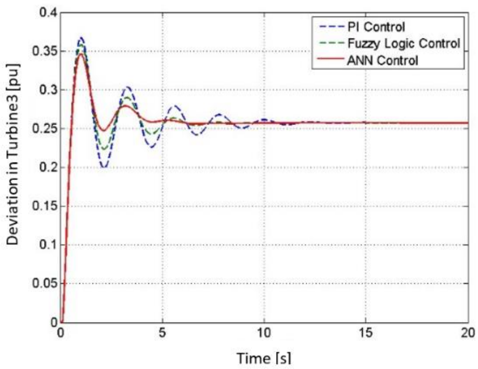

Fig. 12. Deviation of TURBINE3 power.

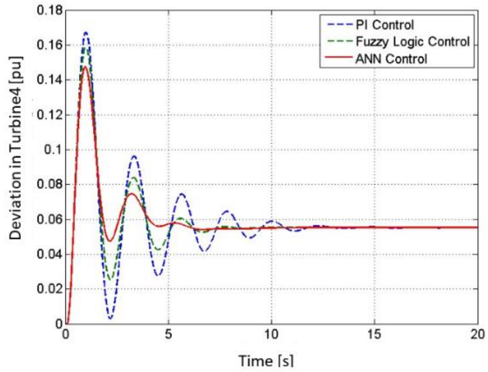

Fig. 13. Deviation of TURBINE4 power.

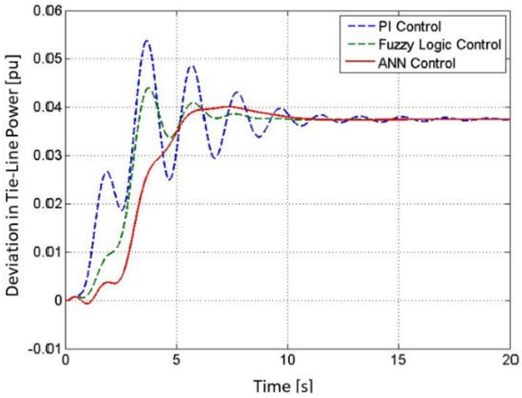

Fig. 14. Deviation of Tie-Line power flow.

When comparing load frequency control shown in Table 2 strategies in terms of rise time, settling time, and peak overshoot, certain characteristics emerge. PI control, a classic strategy, offers reasonable rise time and settling time, but it may exhibit some peak overshoot in response to sudden load changes. Fuzzy logic control, leveraging linguistic variables and rules, provides fast rise time, satisfactory settling time, and effective mitigation of peak overshoot by adapting to uncertainties. ANN control, utilizing artificial neural networks, can deliver fast rise time and good settling time, with the ability to learn from training data to reduce peak overshoot.

Table 2. Comparative results of load frequency control strategies.

Performance metric	ANN Control	Fuzzy Logic control	PI control
Rise time [s]	0.96	1.57	2
Settling time [s]	1.27	2.1	2.36
Overshoot [m/s]	0.07	0.16	0.31
Steady-state error [m/s]	3.6	4.12	6.39

Fuzzy logic control and ANN control, with their capabilities to handle nonlinearities and uncertainties, have the potential to outperform PI control. However, the selection of the most suitable strategy depends on system characteristics, tuning parameters, available training data, and the expertise of the control engineer. Proper evaluation and tuning are crucial to choosing the optimal control strategy for a specific load frequency control scenario.

4.1. Optimization by using PSO for load allocation with each generation station

As shown in Table 3, which represents the inertia weight in the PSO algorithm. The inertia weight (w) controls the balance between exploration and exploitation during the optimization process. c1 and c2- These are the cognitive coefficient and social coefficient, respectively, used in the Particle Swarm Optimization (PSO) algorithm. ev_mean- It refers to the mean value of the Electric Vehicle (EV) charging load deviation. ev_std-. The standard deviation quantifies the dispersion or variability of the EV charging load values around the mean.

A compararison of the load distribution results for two different combinations of EV charging load deviation is shown in Table 4. EV charging load deviation with mean = 1 and standard deviation = 0.1: with EV charging load deviation with mean = 1 and standard deviation = 0.5. Comparing the two cases, we can observe that when the standard deviation is higher (0.5), the load distribution values for each GENCO are generally higher compared to when the standard deviation is lower (0.1).

This higher variability in the EV charging load results in a wider range of load values assigned to each GENCO. On the other hand, when the standard deviation is lower (0.1), the load distribution values are generally lower for each GENCO, indicating less variability in the EV charging load and a more consistent load assignment among the GENCOs. The choice of the mean and standard deviation for the EV charging load deviation depends on the specific characteristics of the EV charging load in the given scenario, including the level of uncertainty and variability expected in the charging behavior.

Table 3: PSO Parameters.

Parameter	Value
Number of particles	10
Max iterations	100
w	2
c1	4
c2	4

Table 4: Deviation in load distribution.

Parameter	ev_mean 0.2	ev_mean 0.4	ev_mean 0.6	ev_mean 0.8	ev_mean 1	1 with ev_std 0.5
GENCO 1 [pu MW]	0.0615	0.0880	0.0980	0.1080	0.0980	0.1180
GENCO 2 [pu MW]	0.0799	0.0902	0.1002	0.1102	0.1002	0.1202
GENCO 3 [pu MW]	0.1031	0.0979	0.1079	0.1179	0.1079	0.1279
GENCO 4 [pu MW]	0.0196	0.0780	0.0880	0.0980	0.1079	0.1080

From the comparison in Table 5, we can observe that there are differences in the load distribution values obtained from the PSO algorithm [12] and the GA algorithm. Specifically, we see variations in the load assigned to each GENCO. For example, in the case of GENCO 1, the PSO algorithm assigns a load of 0.0980 pu MW, while the GA algorithm assigns a slightly higher load of 0.1026 pu MW. Similarly, for other GENCOs, we can see variations in the load distribution values between the two algorithms. These differences in load distribution can be attributed to the distinct optimization approaches and mechanisms employed by the PSO and GA algorithms. Each algorithm has its own way of exploring and exploiting the search space, which can lead to divergent results in terms of load allocation. Ultimately, the choice between the PSO algorithm and the GA algorithm would depend on the specific requirements of the problem, including factors such as convergence speed, solution quality, and computational efficiency.

Table 5: Comparison of PSO and GA.

GENCO	PSO Algorithm [pu MW]	GA Algorithm [pu MW]
GENCO 1	0.0980	0.1026
GENCO 2	0.1002	0.1088
GENCO 3	0.1079	0.0967
GENCO 4	0.0880	0.0923

The load distribution and allocation of resources among the generation units, as determined by the load distribution algorithms like PSO or GA, can have an impact on economic load dispatch (ELD). Economic load dispatch is the process of allocating the generation output among the available units in a power system to meet the load demand while minimizing the total operating cost. When the load distribution among the generation units is optimized using algorithms like PSO or GA, it affects the input parameters for the economic load dispatch problem. The allocated load to each generation unit, along with their associated costs, determines the total cost of generation. By optimizing the load distribution, the operating cost of the system can be minimized, leading to more efficient and cost-effective operation. Therefore, the load distribution results obtained from algorithms like PSO or GA can serve as valuable inputs to the economic load dispatch problem, allowing for better management of generation resources and improved cost efficiency.

5. CONCLUSIONS

The load distribution results obtained from the Particle Swarm Optimization (PSO) algorithm and the Genetic Algorithm (GA) for the given EV charging load deviation parameters (ev_mean = 1 and ev_std = 0.1) highlight the variability in load allocation among the GENCOs. With their distinct optimization approaches, PSO and GA exhibit differences in load distribution values. We observed distinct variations in the load allocation to each

GENCO. For instance, in the context of GENCO 1, the PSO algorithm assigns a load of 0.0980 pu MW, while the GA algorithm slightly increases it to 0.1026 pu MW. Similarly, other GENCOs exhibit differing load distribution values due to the unique optimization mechanisms of PSO and GA. These disparities are to be attributed to the fundamental differences in how the two algorithms approach the optimization task.

REFERENCES

[1] K. Musa, H. Sun, Y. Xiang, D. Shi, "Electric vehicles participation in load frequency control based on mixed $H2/H_\infty$," *International Journal of Electrical Power & Energy Systems,* vol. 125, p. 106420, 2021, doi: 10.1016/j.ijepes.2020.106420.

[2] A. Khalil, Z. Rajab, A. Alfergani, O. Mohamed, "The impact of the time delay on the load frequency control system in microgrid with plug-in-electric vehicles," *Sustainable cities and society*, vol. 35, pp. 365-377, 2017, doi: 10.1016/j.scs.2017.08.012.

[3] Z. Farooq, R. Asadur, S. Lone. "Load frequency control of multi-source electrical power system integrated with solar-thermal and electric vehicle," *International Transactions on Electrical Energy Systems,* vol. 31, no. 7, doi: 10.1002/2050-7038.12918.

[4] T. Pham, H. Trinh, L. Hien, "Load frequency control of power systems with electric vehicles and diverse transmission links using distributed functional observers," *IEEE Transactions on Smart Grid,* vol. 7, no. 1, pp. 238-252, 2015, doi: 10.1109/TSG.2015.2449877.

[5] Y. Arya, "Effect of electric vehicles on load frequency control in interconnected thermal and hydrothermal power systems utilising CF-FOIDF controller." *IET Generation, Transmission & Distribution*, vol. 14, no. 14, pp. 2666-2675, 2020, doi: 10.1049/iet-gtd.2019.1217.

[6] Y. Li, Q. Zhang, C. Li, "Real-time adjustment of load frequency control based on controllable energy of electric vehicles," *Transactions of the Institute of Measurement and Control*, doi: 10.1007/978-981-13-2381-2_10.

[7] A. Dutta, P. Surya, "Utilizing electric vehicles and renewable energy sources for load frequency control in deregulated power system using emotional controller," *IETE Journal of Research*, vol. 68, no. 2, pp. 1500-1511, 2019, doi: 10.1080/03772063.2019.1654936.

[8] Y. Tang, J. Yang, J. Yan, H. He, "Intelligent load frequency controller using GrADP for island smart grid with electric vehicles and renewable resources," *Neurocomputing,* vol. 170, pp. 406-416, 2015, doi: 10.1016/j.neucom.2015.04.092.

[9] A. Naveed, S. Şahi, A. Saffe, "Impact of electric vehicle aggregator with communication time delay on stability regions and stability delay margins in load frequency control system," *Journal of Modern Power Systems and Clean Energy,* vol. 9, no. 3, pp.595-601, doi: 10.35833/MPCE.2019.000244.

[10] M. Khooban, T. Niknam, F. Blaaberg, T. Dragičević, "A new load frequency control strategy for micro-grids with considering electrical vehicles," *Electric Power Systems Research*, vol. 143, pp. 585-598, 2017, doi: 10.1016/j.epsr.2016.10.057.

[11] D. Aravindh, R. Sakthivel, B. Kaviarasan, S. Anthoni, F. Alzahrani, "Design of observer-based non-fragile load frequency control for power systems with electric vehicles," *ISA transactions,* vol. 91, pp. 21-31, doi: 0.1016/j.isatra.2019.01.031.

[12] A. Safari, B. Farshad, F. Meisam, "A load frequency control using a PSO-based ANN for micro-grids in the presence of electric vehicles," *International Journal of Ambient Energy,* vol 42, no. 6, pp. 688-700, 2021, doi: 10.1080/01430750.2018.1563811.